

# Numerical modelling of soil-foundation interaction by a new non-linear macro-element

Mourad Khebizi<sup>\*1</sup>, Hamza Guenfoud<sup>2</sup> and Mohamed Guenfoud<sup>2</sup>

<sup>1</sup>Department of Civil Engineering, Mentouri University of Constantine, Algeria

<sup>2</sup>Civil Engineering and Hydraulic Laboratory, University of Guelma, Algeria

(Received December 8, 2016, Revised August 13, 2017, Accepted August 23, 2017)

**Abstract.** This paper focuses on the development of a new non-linear macro-element for the modelling of soil-foundation interaction. Material and geometrical nonlinearities (soil yielding and foundation uplift respectively) are taken into account in the present macro-element to examine the response of shallow foundations under monotonic and cyclic loads. Several applications of soil-foundation systems are studied. The results obtained from these applications are in very favourable agreement with those obtained through other numerical models in the literature.

**Keywords:** numerical modelling; macro-element; soil-footing systems; interaction; non-linear; cyclic loads

## 1. Introduction

The non-linear behaviour of shallow foundations is a major objective for civil engineering researchers. On the one hand, the nonlinearities of rigid shallow foundations are related to the soil plasticity under a foundation and, on the other hand, to the uplift of the soil–foundation interface (Lu *et al.* 2016, Gazetas 2015, Anastasopoulos and Kontoroupi 2014, Bhaumik and Raychowdhury 2013, Gazetas *et al.* 2013, Gelagoti *et al.* 2012). They are not only related to the nature of the materials (soils+foundations) (Khebizi 2015, Khebizi and Guenfoud 2015), but also to the type of loading. The latter can be static, cyclic, or dynamic; they cause vertical displacement, horizontal displacement and rotation of the foundations (Fig. 1). Foundation systems are also subject to the action of seismic solicitations and are damaged, sometimes with very serious consequences for the structures (Gelagoti *et al.* 2012, Chatzigogos 2007). The conventional methods of calculation or those that give the current codes are insufficient to provide a reliable representation of the response of shallow foundations when the soil–foundation interaction is taken into account.

In this paper, we present a simplified and reliable numerical modelling method which is able to take into account the soil–foundation interaction by considering all nonlinearities associated with foundation uplift and with soil yielding. The method uses a “gap” element connected in a series with a “non-linear link that follows Wen plasticity” (Wen 1976) in order to form a new macro-element. The horizontal behaviour of the foundation is controlled by a non-linear horizontal link. The soil-foundation system can be modelled by a single macro-element located in the footing centre, as it can be modelled

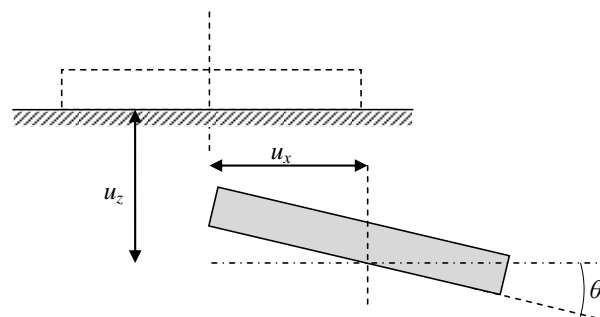


Fig. 1 Two-dimensional response of a rigid shallow foundation

by a rigid beam resting on a set of the vertical macro-elements according to the Winkler approach (see Section 3).

## 2. Presentation of the macro-element

The macro-element developed in this work is a “gap” element connected in a series with a non-linear link (Fig. 6). This macro-element is able to describe the material and geometrical nonlinearities.

The “gap” element (Fig. 2) is used to simulate the footing uplift. This element carries compression loads only; it has zero stiffness when subjected to tension. The non-linear force–displacement relationship is given by

$$F = \begin{cases} k_g (u + open) & \text{if } u + open > 0 \\ 0 & \text{otherwise} \end{cases} \quad (1)$$

where  $k_g$  is the spring constant, and  $open$  is the initial gap opening, which must be zero or positive, and  $u$  the displacement (positive in compression).

The non-linear link (Fig. 4) is used to simulate the soil plasticity under the foundation. The plasticity model is

\*Corresponding author, Professor  
E-mail: Mourad\_gc@yahoo.fr

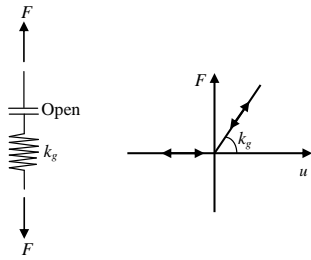


Fig. 2 Structure and behaviour of the “gap” element

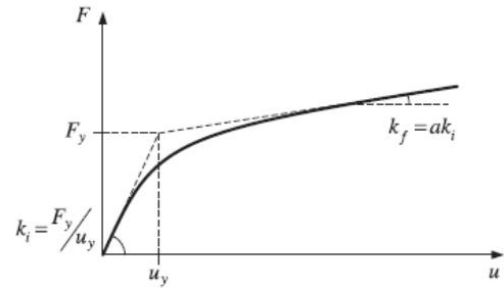


Fig. 5 Behaviour of the Wen model

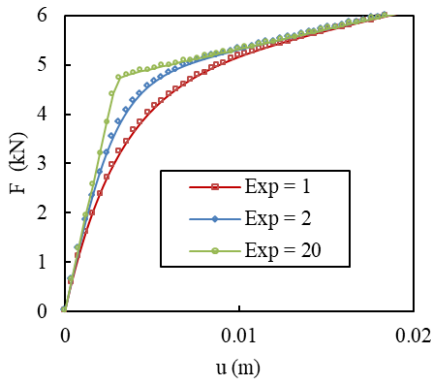
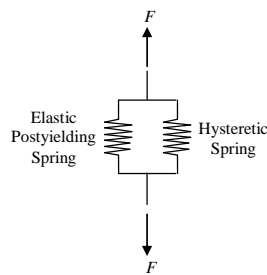
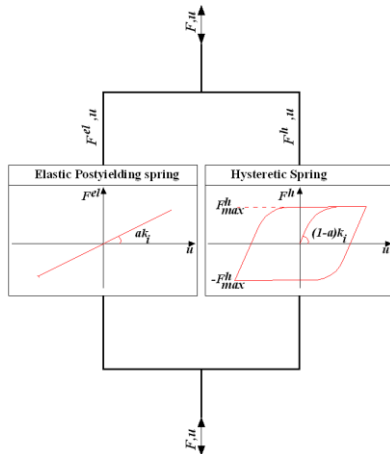


Fig. 3 Sharpness of yielding



(a) Structure of the Wen model

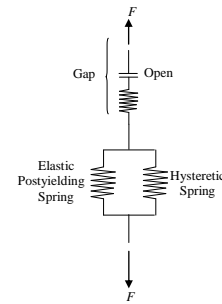


(b) Behaviour of the Wen springs

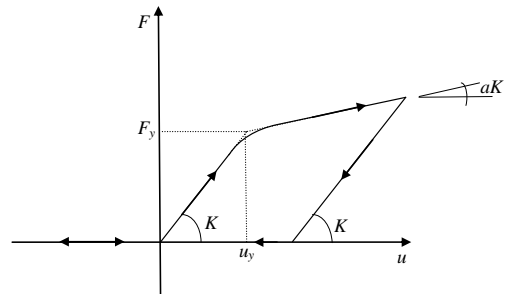
Fig. 4 Structure of the Wen model

based on the hysteretic behaviour proposed by Wen (1976). The nonlinear force-displacement relationship is given by

$$F = a \times \frac{F_y}{u_y} \times u + (1 - a) \times F_y \times z \quad (2)$$



(a) General structure of the macro-element



(b) Behaviour of the macro-element

Fig. 6 General structure and behaviour of the macro-element

where  $u$  is the displacement,  $F_y$  the yield force,  $u_y$  the yield displacement,  $a$  is the ratio of post-yield to pre-yield (elastic) stiffness, and  $z$  is a dimensionless hysteretic parameter that obeys to single non-linear differential equation with zero initial condition

$$\dot{z} = \frac{k_i}{F_y} \begin{cases} \dot{u}(1 - |z|^{\exp}) & \text{if } \dot{u}z > 0 \\ \dot{u}(t) & \text{otherwise} \end{cases} \Rightarrow z = \frac{1}{u_y} \begin{cases} \dot{u}(1 - |z|^{\exp}) & \text{if } \dot{u}z > 0 \\ \dot{u} & \text{otherwise} \end{cases} \quad (3)$$

where  $\exp$  is an exponent greater than or equal to unity. Larger values of this exponent increase the sharpness of yielding, as shown in Fig. 3. The practical limit for  $\exp$  is about 20. The equation for  $\dot{z}$  is equivalent to Wen’s model (see Eq. (4)) with  $A = 1$  and  $\alpha = \beta = 0.5$ .

$$\dot{z} = \frac{1}{u_y} \left[ A - |z|^{\exp} \left( \beta + \text{sgn}(\dot{u}z)\alpha \right) \right] \dot{u} \quad (4)$$

where  $A$ ,  $\alpha$  and  $\beta$  are dimensionless quantities controlling the behaviour of the model,  $\text{sgn}(\bullet)$  is the signum function.

It follows from Eq. (2) that the restoring force  $F$  can be divided into an elastic and a hysteretic part as follows

$$F^{el} = a \times \frac{F_y}{u_y} \times u \quad (5)$$

$$F^h = (1-a) \times F_y \times z \quad (6)$$

Thus, the model can be visualised as two springs connected in parallel (Fig. 4) where  $k_i = F_y/u_y$  and  $k_f = ak_i$  are the initial stiffness and post-yielding stiffness of the system, respectively.

Fig. 6 shows the general structure of the non-linear macro-element. The behaviour law associated with this macro-element is not symmetrical (Fig. 6) and is characterised, on one hand, by a yield load in compression  $F_y$ , and, on the other hand, by a reduction of the recall force as the foundation is uplifted. The recall force is finally approaches zero.

The global elastic stiffness  $K$  of the macro-element is calculated as follows

$$\frac{1}{K} = \frac{1}{k_g} + \frac{1}{k_i} \Rightarrow K = \frac{k_g \times k_i}{k_g + k_i} \quad (7)$$

Gazetas (1991) has developed equations that allow the computation of this stiffness according to the foundation shape and function of the soil characteristics.

The yield load in compression is given by the following relationship adapted to a rectangular foundation (Davis and Booker 1973, Matar and Salençon 1979, Philipponnat and Hubert 2003)

$$F_y = \left[ \left(1 - 0.2 \frac{B}{L}\right) \gamma \frac{B}{2} N_\gamma + q_0 N_q + \left(1 + 0.2 \frac{B}{L}\right) c N_c \right] BL \quad (8)$$

where  $q_0$  is the effective vertical stress brought by the soil at the base of the foundation,  $\gamma$  is the soil unit weight,  $N_\gamma$ ,  $N_q$ , and  $N_c$  are the bearing capacity factors, which are functions of the soil friction angle. The relationships that allow the calculation of these factors are given in Caquot and Kérisel (1966). Recently, Dixit *et al.* (2013) have shown that the bearing capacity factor  $N_\gamma$  decreases by increasing the footing dimensions. Several experimental investigations have also been undertaken to study the bearing capacity (Smith-Pardo 2014, Mohamed *et al.* 2013).

### 3. Vertical stiffness distribution

Many results of experimental works conducted on shallow foundations under cyclic loading highlight that at the time of the rocking phenomenon, the soil tends to settle and densify at the edges of the footing. This is explained by the fact that when one of the ends is uplifted, the other is heavily loaded. The stiffness at the ends of the foundation is thus found to be higher than that in the centre (the stiffness in the end regions may increase due to densification). In order to take into account this behaviour in a Winkler-type modelling, it is possible to associate the degree of soil densification with the degree of coupling that exists between the vertical and rotational stiffness of the system. To reach this goal, FEMA 356 (American Society of Civil Engineers [ASCE] 2000) has adopted a simplified method

to take into account this coupling. A non-uniform distribution of the vertical stiffness of the springs is recommended as shown in Fig. 7. The footing is divided into two regions: end region to represent the effect of the rotational stiffness and middle region to represent the vertical stiffness. The middle region stiffness intensity  $k_{mid}$  is taken as that for an infinitely long strip footing (i.e.,  $L/B \rightarrow \infty$ ). The end region vertical stiffness intensity  $k_{end}$  is based on the vertical stiffness of an isolated plate with an area of  $B \times B/6$ . The resulting stiffness intensities using Gazetas' (1991) equations are

$$k_{mid} = \frac{0.73G}{(1-\nu)B} \quad (9)$$

and

$$k_{end} = \frac{6.83G}{(1-\nu)B} \quad (10)$$

where  $G$  is the shear modulus and  $\nu$  is Poisson's ratio.

Finally, this stiffness variation along the foundation implicitly gives this system a rotational stiffness. In addition to this vertical stiffness variation along the foundation, the method recommends bringing the springs at the end zones closer if the studied systems are strongly dominated by the foundations rocking.

From this method, Harden *et al.* (2005) have developed a more rigorous way to estimate  $k_{mid}$  and  $k_{end}$ . Whereas, in FEMA 356 (2000) the length of the end regions  $L_{end}$  is constant and equal to  $B/6$ . The method given by Harden assumes that  $L_{end}$  is a function of the  $B/L$  ratio, this method is based on the assumption that the length  $L_{end}$  is controlled by the value of the rotational stiffness which is not provided by the vertical stiffness intensity-in other words, by their degree of coupling. In the case, a parameter  $C_{R-\nu}^K$  is used to take into account the rotational stiffness deficiency of the system and the coupling between the vertical and the rotational stiffness, as given by the following expression

$$C_{R-\nu}^K = \frac{K_{\theta_y} - \frac{K_z}{BL} I_y}{K_{\theta_y}} \quad (11)$$

where  $B$  and  $L$  is the foundation dimensions,  $I_y = BL^3/12$  is the moment of inertia.

If  $C_{R-\nu}^K$  is equal to zero,  $K_z$  and  $K_{\theta_y}$  are not coupled. In this case, the stiffness intensity is constant over the entire length of the foundation and equal to  $k$ , where

$$k = \frac{K_z}{BL} = \frac{K_{\theta_y}}{I_y} \quad (12)$$

In the other case, a greater rigidity is required at the ends so that the rotational global stiffness of the system is well represented. Where  $L_{end}$  is given by the following equation (Harden *et al.* 2005)

$$L_{end} = 0.5L - L \left( \frac{1 - C_{R-\nu}^K}{8} \right)^{1/3} \quad (13)$$

Once  $L_{end}$  is defined, the vertical stiffness intensities of the end regions and that of the middle region can be

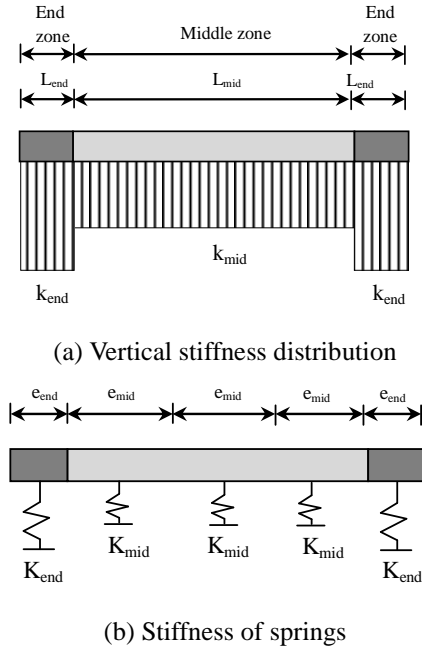


Fig. 7 Simplified method proposed per FEMA 356 (2000)

calculated so that the vertical and the rotational stiffness of the system are equivalent to those of the soil

$$k_{mid} = \frac{K_z}{BL} \quad (14)$$

$$k_{end} = \frac{K_z}{BL} + C_{R-V}^K \frac{K_{\theta y}}{I_y} \quad (15)$$

The stiffness associated with each spring of the model is then obtained by multiplying the stiffness intensity by the tributary area of the spring

$$K_{mid}^{Spring} = k_{mid} B e_{mid} \quad (16)$$

$$K_{end}^{Spring} = k_{end} B e_{end} \quad (17)$$

## 4. Applications

### 4.1 Behaviour of a circular foundation under centred vertical loading

#### 4.1.1 Monotonic loading

In order to see if the macro-element is able to reproduce the behaviour of a foundation under a monotonic static vertical load, we chose to model a circular footing of diameter  $D=1$  m, resting on a layer of clay, whose parameters are  $G=200$  kPa,  $c=1$  kPa and  $\nu=0.5$ .

Houlsby *et al.* (2005) studied analytically and numerically the response of the same foundation. They used the approach of hyperplasticity theory in order to review the modelling potential of the global behaviour of a shallow foundation by adopting Winkler's assumption of decoupled springs. The basic idea is to define a yield surface in terms

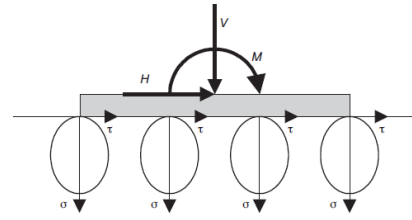


Fig. 8 Generalisation of the Winkler concept (Houlsby *et al.* 2005), considering local models at each point in the soil-foundation interface.

Table 1 Macro-element parameters

Vertical elastic stiffness, $K$	Yield load, $F_y$	Ratio of post-yield, $a$	Exponent, $Exp$
800 kN/m	4.7571 kN	0.001	1

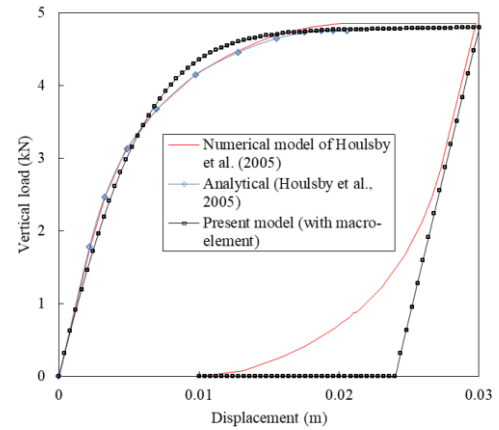


Fig. 9 Vertical load-displacement curve

of the normal and shear stresses ( $\sigma$ ,  $\tau$ ) for each point of the soil-foundation interface. It is a generalisation of the concept of Winkler springs, which defines a local model at any point of the interface. This idea is illustrated in Fig. 8. The global behaviour of the foundation can be obtained by integrating the behaviour at each point on the entire interface. The main assumption of the model is that there are no coupling stress-displacements between two neighbouring points in the soil-foundation interface. The advantage of this assumption is that it allows one to analytically obtain the global behaviour of the foundation.

In our study, the foundation and the subjacent soil are modelled with only one non-linear macro-element localised in the centre of the foundation on which a monotonic vertical displacement is imposed (only one macro-element is sufficient, since only the translation according to the vertical axis is possible and the foundation is considered infinitely rigid). The elastic vertical stiffness of the macro-element is calculated by using the equation developed by Gazetas (1991)

$$K_z = \frac{2GD}{1-\nu} \quad (18)$$

The maximum vertical load supported by the foundation  $F_y$  for a homogeneous cohesive soil is given by

$$F_y = 6.06c \frac{\pi D^2}{4} \quad (19)$$

The numerical parameters of the macro-element are presented in Table 1.

Fig. 9 compares the results obtained with our macro-element and those of Houslyby *et al.* (2005). It can be noted that the non-linear response of the foundation described by the macro-element is practically the same as that described analytically and numerically by Houslyby *et al.* (2005) at the time of the loading phase. Regarding the unloading phase, we noted a discrepancy between the results, as the foundation's response described by the numerical model of Houslyby *et al.* (2005) at the time of the unloading phase after very large displacement produces an unrealistically large uplift of the foundation, as shown in Fig. 9, where there is a very significant decrease of the tangent to the curve in the unloading phase (this is a weakness of Houslyby *et al.*'s model).

Fig. 9 also shows that the macro-element allows a good description of on one hand the material non-linearity of the foundation during the loading phase, and on the other hand the elastic behaviour during unloading, followed by a good description of the foundation uplift (geometrical non-linearity) during the inversion of the loading sign (cancellation of the load by the activation of the gap element). It can be noted that during this loading-unloading cycle, the two components of total displacement are clearly observed, namely elastic and plastic displacements.

#### 4.1.2 Cyclic loading

We will now study the cyclic response of a circular foundation of a diameter  $D=1$  m, resting on a homogeneous cohesive soil. The same foundation has been studied by Chatzigogos (2007) with a numerical series of "swipe tests". Table 2 regroupes the soil characteristics. The maximum vertical load supported by the foundation is given by Eq. (19).

The normalised elastic stiffnesses of the system are calculated with equations from Sieffert and Cevaer (1992) and Chatzigogos (2007)

$$K_z = \frac{2GD^2}{F_y(1-\nu)} \quad (20)$$

$$K_x = \frac{4GD^2}{F_y(1-\nu)} \quad (21)$$

$$K_\theta = \frac{GD^2}{3F_y(1-\nu)} \quad (22)$$

In this paper, the soil-foundation system is modelled by a non-linear macro-element localised in the centre of the foundation. The normalised elastic stiffnesses of this macro-element are calibrated compared to the numerical "swipe tests" conducted by Chatzigogos (2007) with a monotonic vertical load. Fig. 10 shows a comparison of the foundation response under a monotonic centred loading obtained with the present macro-element and that obtained by Chatzigogos (2007) with numerical tests. It is observed that

Table 2 Soil characteristics

Soil cohesion, $c_0$	Shear modulus, $G$	Poisson's ratio, $\nu$	Soil unit weight, $\gamma$	Yield load, $F_y$
1 kPa	1000 kPa	0.3	20 kN/m <sup>3</sup>	4.76 kN

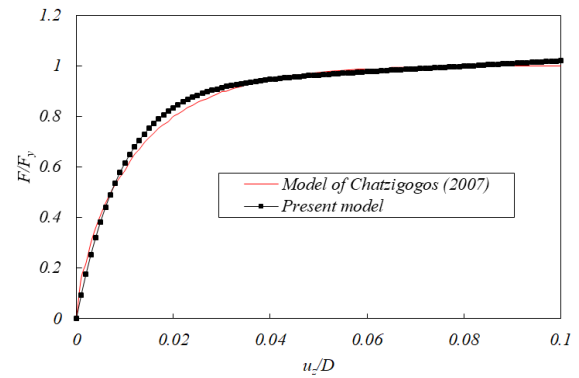


Fig. 10 System response under monotonic loading

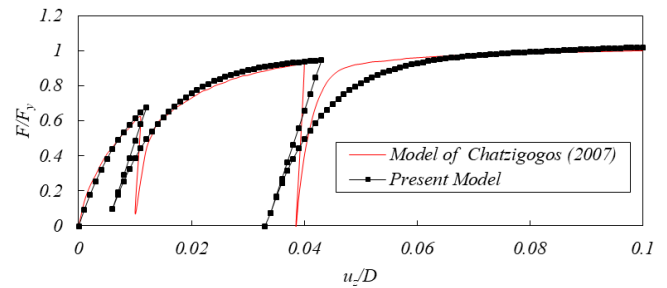


Fig. 11 System response under cyclic loading (loading-unloading-reloading)

the two results are identical.

Thereafter, cyclic loading controlled by displacements is applied to the foundation (loading-unloading-reloading).

Fig. 11 shows the path of the foundation response in terms of the generalised parameters ( $F/F_y$ ,  $u_z/D$ ), and compares the results obtained with the present macro-element and those of Chatzigogos (2007). We note that for the loading and reloading phases, our results are very close to those to the numerical tests, and it can be clearly observed that the response produced by our macro-element in the reloading phase has the same trend, as in the first loading response. However, the response produced by the numerical tests in the reloading phase is considerably different from that in the first loading phase.

As for as the unloading phase is concerned, a certain difference between the two results is observed, where we noted that the model of Chatzigogos (2007) is quasi rigid in the unloading phase (the elastic stiffness is almost infinite), while the unloading stiffness of our macro-element is the same as the elastic stiffness in the loading phase.

Then, it can be seen that the macro-element developed in this paper is able to reproduce the non-linear behaviour of a circular foundation under monotonic and cyclic loading.

#### 4.2 Behaviour of a circular foundation under horizontal loading

In order to study the behaviour of a shallow foundation

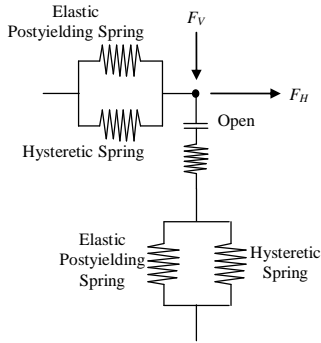
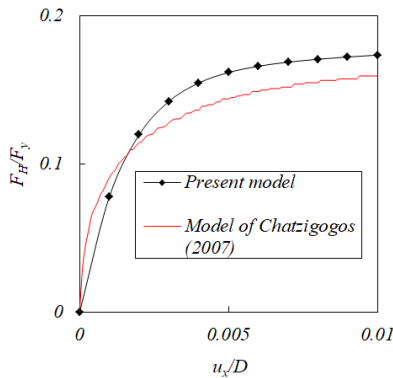
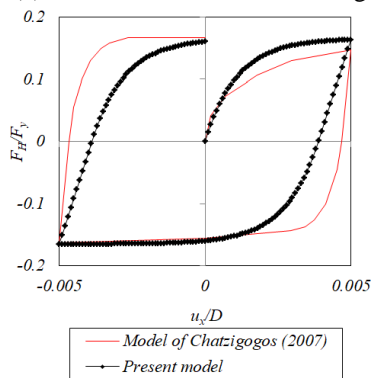


Fig. 12 Numerical model of the soil–foundation system



(a) Monotonic horizontal loading



(b) A cyclic horizontal loading

Fig. 13 System response under horizontal loading

under monotonic and cyclic horizontal loading, the “swipe tests” carried out by Chatzigogos (2007) have also been used. In this case the foundation is initially subjected to a vertical displacement which brings the system to a certain level of yielding. Then, a horizontal displacement is applied until collapse.

The numerical model of the soil-foundation system is shown in Fig. 12, in which we modelled the vertical behaviour by the macro-element developed previously and presented on Fig. 6. With regard to the horizontal behaviour of the system, a horizontal macro-element is used in which the model of plasticity is based on the hysteresis behaviour proposed by Wen (1976) (Figs. 4 and 5). The maximum horizontal load of the macro-element is given by Chatzigogos *et al.* (2009)

$$F_y^H = c_0 A \tag{23}$$

where  $A$  is the area of the foundation.

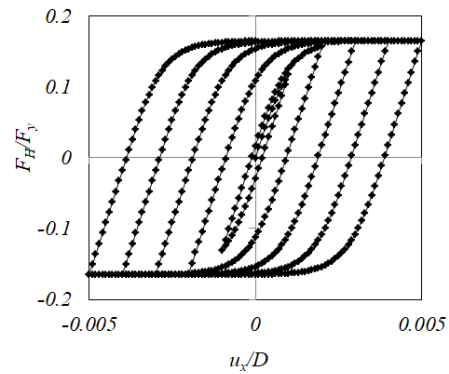
The results presented in this section are relative to the curves of the horizontal response of the foundation under monotonic and cyclic loading (one cycle and five cycles), respectively, in terms of normalised parameters ( $F_H/F_y$ ,  $u_x/D$ ). The displacement history defined for each case is as follows:

In the first case (Fig. 13(a)), a vertical displacement of  $u_z=0.03$  m is initially applied. Then the vertical displacement is kept constant and a horizontal displacement is incrementally applied upto the value of  $u_x=0.01$  m.

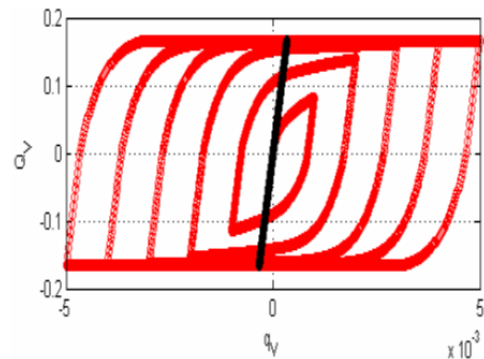
In the second case (Fig. 13(b)), a vertical displacement of  $u_z=0.01$  m is applied, which brings the system to a value of  $F_v/F_y=0.6$ . Then, a perfect cycle (loading-unloading-loading negative-unloading) is applied while arriving at a value of  $u_x=\pm 0.005$  m.

In the third case (Figs. 14(a) and 14(b)), the test is initiated by the application of a vertical displacement equal to  $u_z=0.01$  m. Then, five cycles of horizontal loading are applied. In each new cycle, the horizontal displacement applied is increased linearly. For the first cycle there is  $u_x=\pm 0.001$  m and for the fifth one it reaches  $u_x=\pm 0.005$  m. The diagram of  $F_H/F_y-u_x/D$  shows that each new cycle contains the preceding cycles, which are less important.

It is finally noted, that the numerical model of our investigation allows a description of the system non-linear behaviour, for the monotonic horizontal loading as well as for cyclic horizontal loading. A good agreement with the tests carried out by Chatzigogos (2007) is observed. Nevertheless, certain differences are found, especially for the unloading phases.



(a) Present model



(b) Model of Chatzigogos (2007)

Fig. 14 System response under cyclic horizontal loading (five cycles)

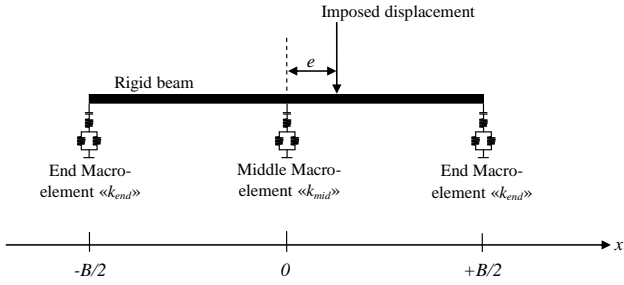


Fig. 15 Numerical model of the foundation: rigid beam resting on 3 macro-elements

Table 3 Soil characteristics

Soil unit weight, $\gamma$	Internal friction angle of soil, $\varphi$	Poisson's ratio, $\nu$	Shear modulus, $G$
20 kN/m <sup>3</sup>	35°	0.35	29630 kPa

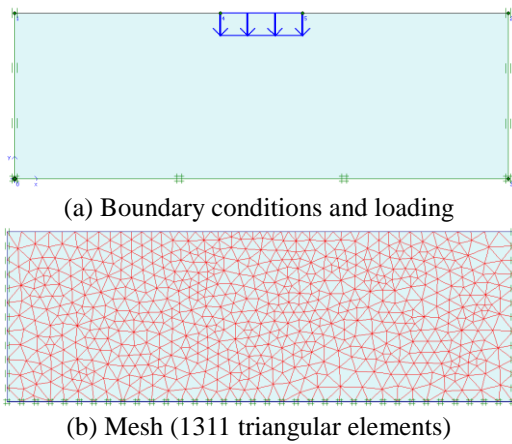


Fig. 16 Finite elements model with Plaxis code

Table 4 Foundation characteristics

Elastic stiffness of foundation $K_z$	78000 kN/m
Yield load of the foundation $F_y$	360.9 kN

Table 5 Parameters of the macro-elements

Parameters of the macro-elements	Uniform repartition	Harden repartition
Tributary area of the middle macro-element $B \times L_{mid}$	1 m × 0.5 m	1 m × 0.74 m
Tributary area of the end macro-element $B \times L_{end}$	1 m × 0.25 m	1 m × 0.13 m
Stiffness of the middle macro-element $k_{mid}$	39000 kN/m	57783 kN/m
Stiffness of the end macro-element $k_{end}$	19500 kN/m	24865 kN/m
Ratio of post-yield (for all macro-elements) $\alpha$	0.001	0.001
Exponent (for all macro-elements) $Exp$	2	2

### 4.3 Behaviour of a strip footing under monotonic eccentric loads

In this section, we will study the non-linear behaviour of a strip foundation with a width of  $B=1$  m, resting on a purely frictional soil. Table 3 summarises the soil parameters. A monotonic imposed displacement is applied to several eccentricities from the foundation centre (the loading in imposed displacements permits a direct investigation of the failure criterion to be conducted).

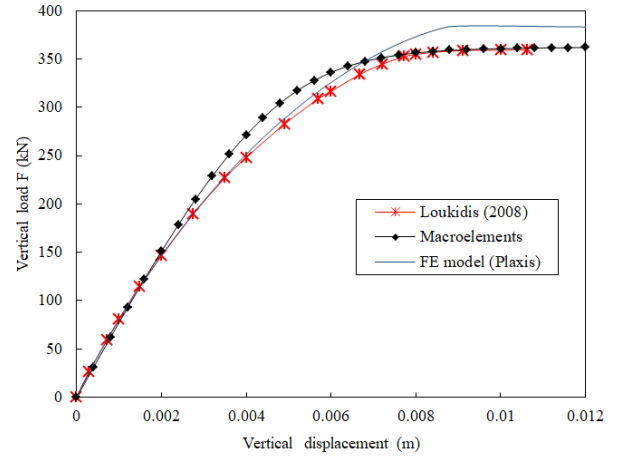
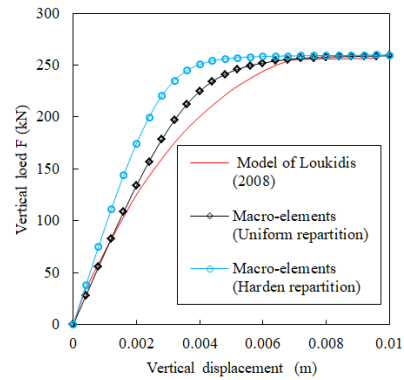
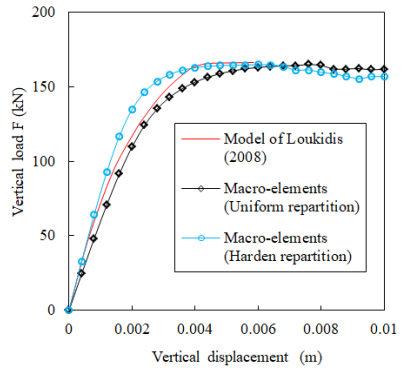


Fig. 17 Load-displacement curve for a null eccentricity



(a) Response for eccentricity  $e=B/12$

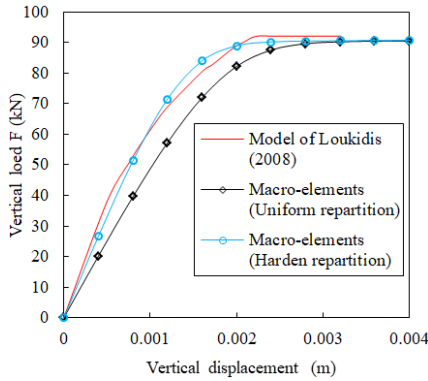


(b) Response for eccentricity  $e=B/6$

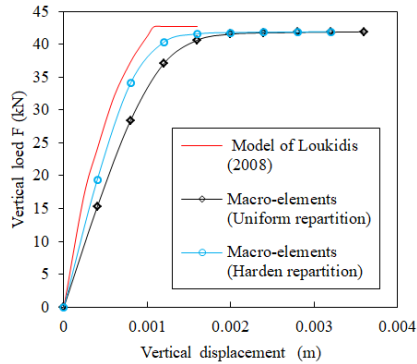
Fig. 18 Load-displacement curve for eccentricity,  $e=B/12$  and  $e=B/6$

Loukidis (2008) has also analysed the behaviour of the same foundation under a vertical static loading of increasing intensity applied to several eccentricities. He used the finite elements method to model the soil and the foundation with the SNAC code developed by Abbo and Sloan (2000). In his modelling, Loukidis has ignored the uplifting of the foundation (no interface element between the foundation and the soil was used), and he only takes into account the soil plasticity with an elastic-perfectly plastic behaviour following the Mohr-Coulomb failure criterion.

In this work, we model the foundation with a rigid beam resting on three independent non-linear macro-elements (Fig. 15), where the material and geometric nonlinearities are considered. The vertical stiffness of the soil-foundation



(a) Response for eccentricity  $e=B/4$



(b) Response for eccentricity  $e=B/3$

Fig. 19 Load-displacement curve for eccentricity,  $e=B/4$  and  $e=B/3$

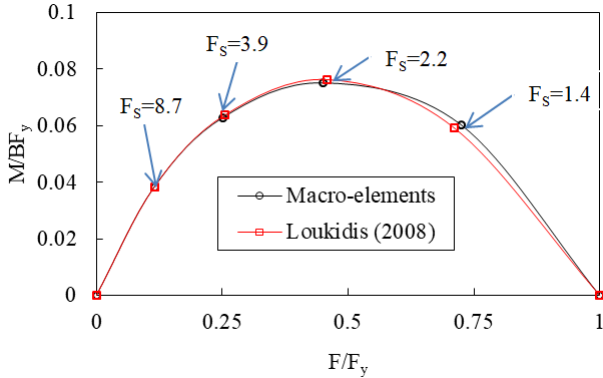
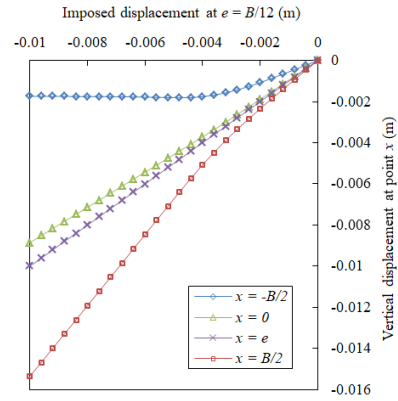


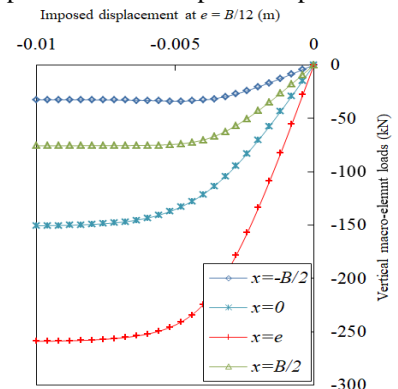
Fig. 20 Envelope of the normalised moment-vertical load interaction

system is distributed through two methods: in the first one, we consider that it is uniformly distributed along the foundation, and in the second method, we use a non-uniform distribution of the vertical stiffness macro-elements in accordance with the approach of Harden (2005). The following five cases of eccentricity are studied:  $e=0$ ,  $e=B/12$ ,  $e=B/6$ ,  $e=B/4$  and  $e=B/3$ . The parameters of the foundation and the macro-elements are shown in Tables 4 and 5, respectively.

For reasons of comparison, we also modelled the same foundation (only in the case of a null eccentricity), but this time with the finite element method using the Plaxis code. In this model, the soil is discretised in triangular elements with 15 nodes and the foundation is discretised by an imposed uniform displacement distributed along the width

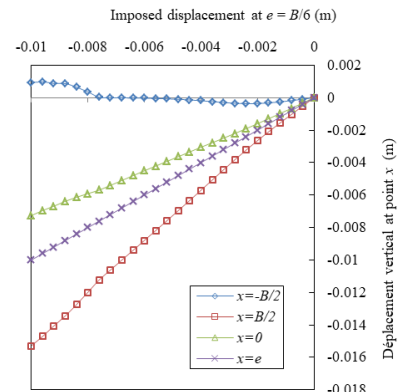


(a) Displacement at  $x$ -imposed displacement curve

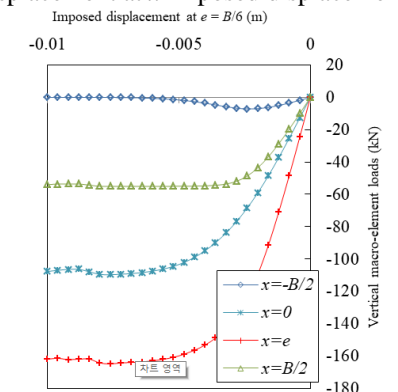


(b) Macro-element load-imposed displacement curve

Fig. 21 Response of the foundation modelled by the macro-elements for the case of  $e=B/12$



(a) Displacement at  $x$ -imposed displacement curve



(b) Macro-element load-imposed displacement curve

Fig. 22 Response of the foundation modelled by the macro-elements for the case of  $e=B/6$

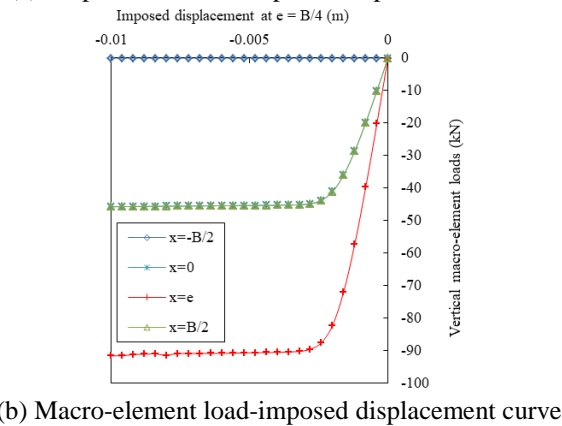
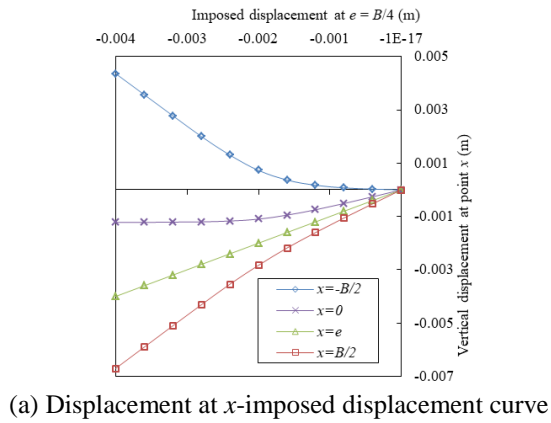


Fig. 23 Response of the foundation modelled by the macro-elements for the case of  $e=B/4$

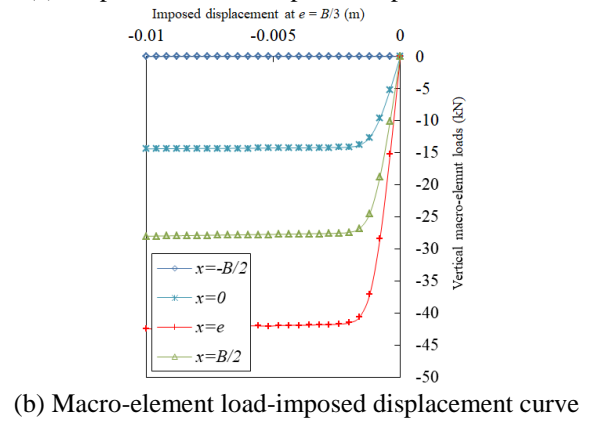
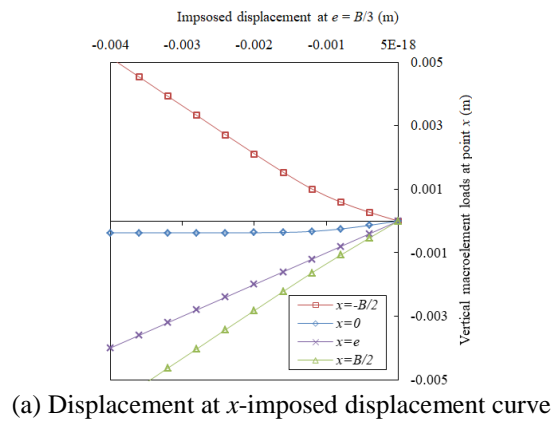


Fig. 24 Response of the foundation modelled by the macro-elements for the case of  $e=B/3$

of the foundation (rigid foundation). The behaviour model used is the Mohr-Coulomb elastoplastic model with an associated flow law. Fig. 16 shows the details of this modelling (boundary conditions, loading, and mesh).

The first results presented are relative to the curve of the vertical load-displacement response for the null eccentricity case. Fig. 17 shows a comparison between the results obtained from our simulations (through macro-elements and FE with Plaxis), with those of Loukidis (2008). We see that our modelling through macro-elements gives generally comparable results to those of Loukidis (2008). However, the small differences between the results can be associated to a mesh effect of the Loukidis model. An agreement between the results obtained by FE (with the Plaxis code) and those of the macro-elements, as well as the results of Loukidis, can be observed. Moreover, a slight difference is noted between the results obtained from the three models. This difference is related to the model size, mesh type, and the load increment.

Figs. 18 and 19 present the non-linear response of the foundation for the eccentricities  $e=B/12$ ,  $e=B/6$ ,  $e=B/4$  and  $e=B/3$ , respectively. We see that the results obtained by our simulation (with macro-elements) are very close to those of Loukidis (2008). However, the small differences between the results are obvious, since Loukidis has ignored the geometric nonlinearities, while all nonlinearities are considered in our modelling with the macro-elements. It is also observed that the stiffness of the soil-foundation system, represented by that of the macro-elements, decreases as the eccentricity increases. This decrease is

caused mainly by the uplift of the foundation.

We also notice a certain difference between the results of two simulations carried out with the macro-elements with a uniform distribution and a non-uniform distribution, where it is can seen that the response of the model described by macro-elements with a non-uniform distribution is more rigid than that obtained by macro-elements with a uniform distribution of vertical stiffness, especially in the case of a low eccentricity ( $e=B/12$ ). In the case of significant eccentricities, a good agreement between the results of the three models is noted. Nevertheless, a slight decrease in system stiffness is observed for the model with a uniform distribution of the macro-elements stiffness.

The diagram in Fig. 20 shows the envelope of the normalised moment-vertical load interaction ( $M/BF_y - F/F_y$ ). It indicates that when the safety factor  $F_s = F_y/F$  is less than 2, the dominant mechanism is that of soil plasticity, but for values of  $F_s$  greater than 2, the uplifting mechanism becomes the dominant one.

Fig. 21 shows that nonlinearities produced for the case of eccentricity  $e=B/12$  are related only to the soil plasticity under the foundation; the foundation uplifting is not observed because of the small loading eccentricity (there is no uplifting, as the vertical load is applied in middle third of the foundation, i.e.,  $e \in [-B/6 B/6]$ ). Fig. 22 also shows that nonlinearities produced for the case of eccentricity  $e=B/6$ , are related to the soil plasticity under the foundation. However, an initiation to foundation uplifting is observed.

Figs. 23 and 24 show that the left end of the foundation ( $x=-B/2$ ) is clearly uplifted when the eccentricity attains

$e=B/4$ . For the case of eccentricity  $e=B/3$ , the percentage of the foundation uplifting is equal to about 50% (i.e., a foundation rotation around its centre).

## 5. Conclusions

In this paper, we proposed a new macro-element oriented to the application of earthquake engineering while insisting on the simplicity of the model. It is able to describe the material nonlinearities associated with soil plasticity, as well as geometric nonlinearities relative to foundation uplifting. Five numerical applications in the literature were studied in order to validate the response of the proposed macro-element under monotonic and cyclic quasi-static loads. The effect of the load eccentricity was also analyzed. According to these applications it was noted that:

- A good agreement exists between the results obtained from the proposed macro-element and those obtained from other numerical models in the literature.
- The nonlinearities of soil-foundation system are well reproduced by the present macro-element.
- The effects of the soil-foundation interaction should be taken into account in the design of the structures.

## References

- Abbo, A.J. and Sloan, S.W. (2000), *SNAC, User Manual, Version 2.0.*, Department of civil, Surveying and Environmental Engineering, University of Newcastle, Callaghan, Australia.
- Allotey, N. and El Naggar, M.H. (2003), "Analytical moment-rotation curves for rigid foundations based on a Winkler model", *Soil Dyn. Earthq. Eng.*, **23**(5), 367-381.
- Allotey, N. and El Naggar, M.H. (2008), "An investigation into the Winkler modeling of the cyclic response of rigid footings", *Soil Dyn. Earthq. Eng.*, **28**(1), 44-57.
- American Society of Civil Engineers (2000), *Prestandard and Commentary for the Seismic Rehabilitation of Buildings (FEMA 356)*, Federal Emergency Management Agency.
- Anastasopoulos, I. and Kontoroupi, T. (2014), "Simplified approximate method for analysis of rocking systems accounting for soil inelasticity and foundation uplifting", *Soil Dyn. Earthq. Eng.*, **56**, 28-43.
- Antoine, L.B. (2009), "Effets du basculement des fondations superficielles sur le comportement sismique des murs de refend en béton armé", Ph.D. Dissertation, Université de Montréal, Montreal, Canada.
- Bhaumik, L. and Raychowdhury, P. (2013), "Seismic response analysis of a nuclear reactor structure considering nonlinear soil-structure interaction", *Nucl. Eng. Des.*, **265**, 1078-1090.
- Caquot, A. and Kérisel, J. (1966), *Traité de Mécanique des Sols*, Gautiers-Villars, France.
- Charalampakis, A.E. and Koumoussis, V.K. (2009), "A Bouc-Wen model compatible with plasticity postulates", *J. Sound Vib.*, **322**(4-5), 954-968.
- Chatzigogos, C.T. (2007), "Comportement sismique des fondations superficielles: Vers la prise en compte d'un critère de performance dans la conception", Ph.D. Dissertation, École Polytechnique, Palaiseau, France.
- Chatzigogos, C.T., Pecker, A. and Salençon, J. (2009), "Macroelement modeling of shallow foundations", *Soil Dyn. Earthq. Eng.*, **29**(5), 765-781.
- Cremer, C., Pecker, A. and Davenne, L. (2001), "Cyclic macroelement for soil-structure interaction: Material and geometrical non-linearities", *J. Numer. Anal. Meth. Geomech.*, **25**(13), 1257-1284.
- Cremer, C., Pecker, A. and Davenne, L. (2002), "Modelling of nonlinear dynamic behavior of a shallow strip foundation with macroelement", *J. Earthq. Eng.*, **6**(2), 175-211.
- Davis, E. and Booker, J. (1973), "The effect of increasing strength with depth on the bearing capacity of clays", *Géotechnique*, **23**(4), 551-563.
- Dixit, M.S. and Patil, K.A. (2013), "Experimental estimate of  $N_y$  values and corresponding settlements for square footings on finite layer of sand", *Geomech. Eng.*, **5**(4), 363-377.
- Gazetas, G. (1991), "Formulae and charts for impedance functions of surface and embedded foundations", *J. Geotech. Eng.*, **117**(9), 1363-1381.
- Gazetas, G. (2015), "4th Ishihara lecture: Soil-foundation-structure systems beyond conventional seismic failure thresholds", *Soil Dyn. Earthq. Eng.*, **68**, 23-39.
- Gazetas, G., Anastasopoulos, I., Adamidis, O. and Kontoroupi, T.H. (2013), "Nonlinear rocking stiffness of foundations", *Soil Dyn. Earthq. Eng.*, **47**, 83-91.
- Gelagoti, F., Kourkoulis, R., Anastasopoulos, I. and Gazetas, G. (2012), "Rocking-isolated frame structures: Margins of safety against toppling collapse and simplified design approach", *Soil Dyn. Earthq. Eng.*, **32**(1), 87-102.
- Harden, C., Hutchinson, T.C., Martin, C.R. and Kutter, B.L. (2005), *Numerical Modeling of the Nonlinear Cyclic Response of Shallow Foundations*, Pacific Earthquake Engineering Research Center.
- Houlsby, G.T., Cassidy, M.J. and Einav, I. (2005), "A generalised Winkler model for the behaviour of shallow foundations", *Géotechnique*, **55**(6), 449-460.
- Khebizi, M. (2015), "Comportement mécanique d'une semelle superficielle sous l'effet d'un séisme", Ph.D. Dissertation, University of Guelma, Guelma, Algeria.
- Khebizi, M., Guenfoud, H. and Guenfoud, M. (2014), "Modélisation des poutres en béton armé par des éléments multicouches", *Courrier du Savoir*, **18**, 111-115.
- Khebizi, M. and Guenfoud, M. (2015), "Numerical modelling of the damaging behaviour of the reinforced concrete structures by multi-layers beams elements", *Comput. Concrete*, **15**(4), 547-562.
- Loukidis, D., Chakraborty, T. and Salgado, R. (2008), "Bearing capacity of strip footings on purely frictional soil under eccentric and inclined loads", *Can. Geotech. J.*, **45**(6), 768-787.
- Lu, Y., Marshall, A.M. and Hajirasouliha, I. (2016), "A simplified Nonlinear Sway-Rocking model for evaluation of seismic response of structures on shallow foundations", *Soil Dyn. Earthq. Eng.*, **81**, 14-26.
- Matar, M. and Salençon, J. (1979), "Capacité portante des semelles filantes", *Revue Française de Géotechnique*, **9**, 51-76.
- Mohamed, F.M.O., Vanapalli, S.K. and Saatcioglu, M. (2013), "Generalized Schmertmann Equation for settlement estimation of shallow footings in saturated and unsaturated sands", *Geomech. Eng.*, **5**(4), 343-362.
- Philipponnat, G. and Hubert, B. (2003), *Fondations et Ouvrages en Terre*, Eyrolles, Paris, France.
- Sieffert, J.G. and Cevaer, F. (1992), *Manuel des Fonctions d'Impédances-Fondations Superficielles*, Presses Académiques.
- Smith-Pardo, J.P. (2012), "Design aids for simplified nonlinear soil-structure interaction analyses", *Eng. Struct.*, **34**, 572-580.
- Smith-Pardo, J.P., Ortiz, A. and Blandon, C.A. (2014), "Biaxial capacity of rigid footings: Simple closed-form equations and experimental results", *Eng. Struct.*, **69**, 149-157.
- Wen, Y.K. (1976), "Method for random vibration of hysteretic systems", *J. Eng. Mech. Div.*, **102**(EM2), 249-263.